

Review

Formalin-Fixed Paraffin-Embedded Tissues—An Untapped Biospecimen for Biomonitoring DNA Adducts by Mass Spectrometry

Byeong Hwa Yun , Jingshu Guo  and Robert J. Turesky * 

Masonic Cancer Center and Department of Medicinal Chemistry, University of Minnesota, 2231 6th St. SE, Minneapolis, MN 55455, USA; bhyun@umn.edu (B.H.Y.); guoj@umn.edu (J.G.)

* Correspondence: rturesky@umn.edu; Tel.: +1-612-626-0141; Fax: +1-612-624-3869

Received: 28 April 2018; Accepted: 25 May 2018; Published: 1 June 2018



Abstract: The measurement of DNA adducts provides important information about human exposure to genotoxic chemicals and can be employed to elucidate mechanisms of DNA damage and repair. DNA adducts can serve as biomarkers for interspecies comparisons of the biologically effective dose of procarcinogens and permit extrapolation of genotoxicity data from animal studies for human risk assessment. One major challenge in DNA adduct biomarker research is the paucity of fresh frozen biopsy samples available for study. However, archived formalin-fixed paraffin-embedded (FFPE) tissues with clinical diagnosis of disease are often available. We have established robust methods to recover DNA free of crosslinks from FFPE tissues under mild conditions which permit quantitative measurements of DNA adducts by liquid chromatography-mass spectrometry. The technology is versatile and can be employed to screen for DNA adducts formed with a wide range of environmental and dietary carcinogens, some of which were retrieved from section-cuts of FFPE blocks stored at ambient temperature for up to nine years. The ability to retrospectively analyze FFPE tissues for DNA adducts for which there is clinical diagnosis of disease opens a previously untapped source of biospecimens for molecular epidemiology studies that seek to assess the causal role of environmental chemicals in cancer etiology.

Keywords: carcinogen; DNA adducts; biomonitoring; formalin-fixed paraffin-embedded tissues; biomarker; mass spectrometry

1. Metabolism, Bioactivation, and DNA Adducts as Biomarkers of Exposure and Health Risk

1.1. Xenobiotic Metabolism and Bioactivation of Procarcinogens

Humans are continuously exposed to potentially hazardous chemicals in the environment, diet, medicines, and through occupational exposures. Many of these chemicals undergo biotransformation by phase I and/or phase II enzymes to produce reactive electrophiles that can form adducts with macromolecules [1]. Cytochrome P450s (P450s) are by far the most important Phase I enzymes involved in xenobiotic metabolism [2]. P450s catalyze a variety of reactions, including aliphatic and aromatic hydroxylation, *N*- or *O*-dealkylation, aliphatic desaturation, hetero atom oxidation, and epoxidation reactions [2]. The resulting metabolites can contain functional groups such as $-OH$, $-NH_2$, and $-SH$ which can undergo conjugation reactions by phase II enzymes, including UDP-glucuronosyltransferases (UGTs), sulfotransferases (SULTs), *N*-acetyltransferases (NATs), glutathione *S*-transferases (GSTs), and methyltransferases [3].

While many Phase I metabolites are detoxification products, some oxidative metabolites are reactive electrophiles, which can induce toxicity or genotoxicity by covalently binding to protein or

DNA, or generate free radicals that deplete cellular antioxidants and induce oxidative stress [4,5]. In a similar vein, many phase II enzyme reactions are regarded as detoxification pathways, and the resulting metabolites are efficiently eliminated from the body. However, in some cases, reactive intermediates are generated, and the metabolites can bind to proteins and DNA. The *O*-acetylation or *O*-sulfation of aromatic amines and heterocyclic aromatic hydroxylamines [6], glutathione conjugation of ethylene dibromide [7], *O*-sulfation of hydroxymethyl polycyclic aromatic hydrocarbons [8], and the acyl glucuronidation of carboxylic acid moieties of nonsteroidal anti-inflammatory drugs (NSAIDs) [9] are examples of conjugation reactions leading to reactive intermediates. The metabolic activation of rodent and possible human carcinogens including 2-amino-1-methyl-6-phenylimidazo[4,5-*b*]pyridine (PhIP) [10], aristolochic acid I (AA-I) [11], 5-methylchrysene [12,13] and tamoxifen [14,15], are shown as examples of procarcinogens that require phase I and/or II enzymes to produce penultimate species that bind to DNA (Figure 1).

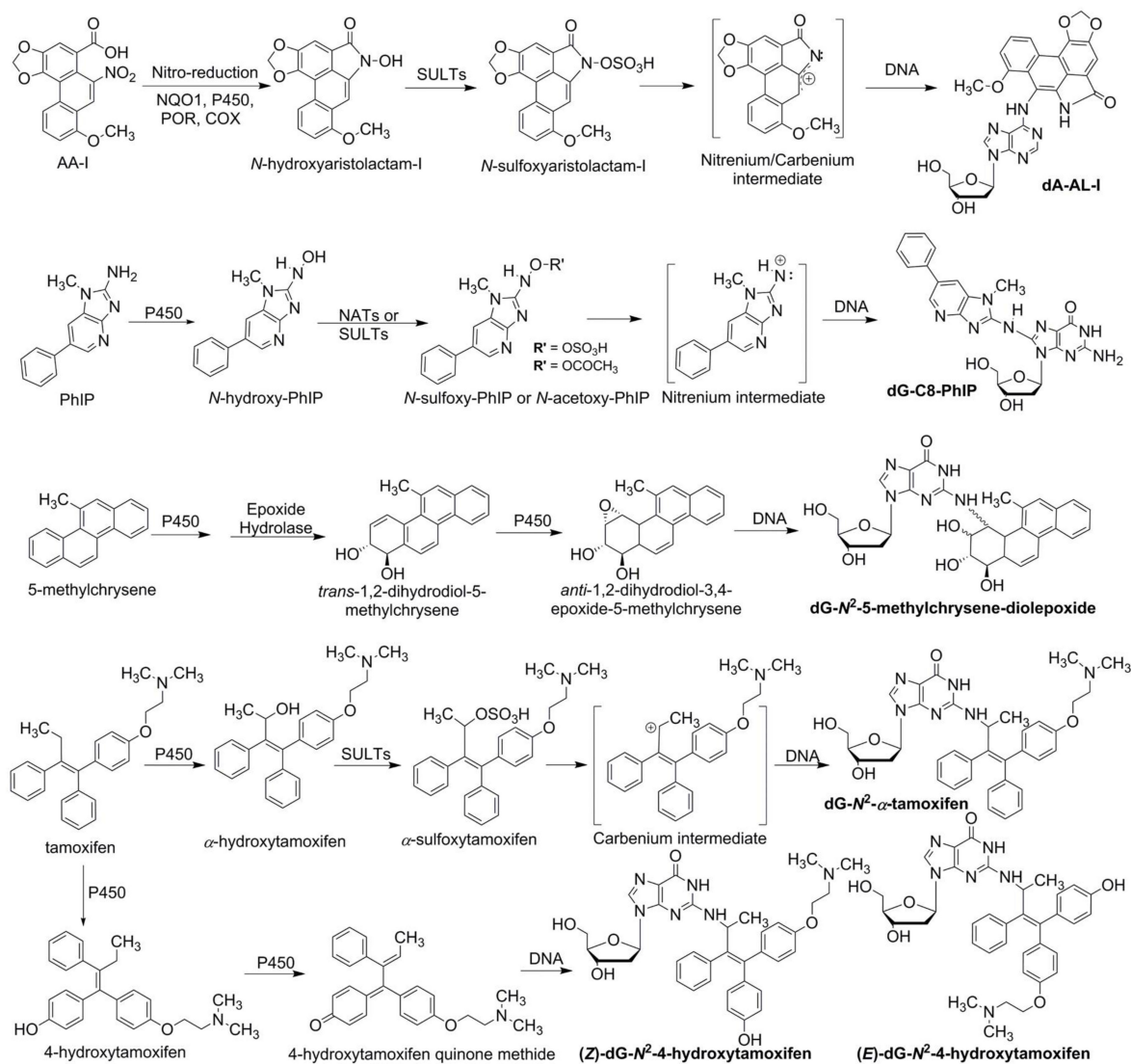


Figure 1. The metabolic activation of aristolochic acid I (AA-I), 2-amino-1-methyl-6-phenylimidazo[4,5-*b*]pyridine (PhIP), 5-methylchrysene, and tamoxifen are shown as prototypes of procarcinogens. Bioactivation is carried out with phase I and/or phase II enzymes, which lead to the formation of DNA adducts. AA-I undergoes nitro-reduction through NAD(P)H:quinone oxidoreductase (NQO1), cytochrome P450s 1A1 and 1A2, NADPH:P450 reductase (POR) or prostaglandin H synthase (COX).

The resulting *N*-hydroxyaristolactam-I is bioactivated by SULTs to form an unstable *N*-sulfoxy ester, which quickly undergoes heterolytic cleavage to produce the reactive nitrenium/carbenium intermediate that forms dA-AL-I and other DNA adducts. PhIP undergoes *N*-hydroxylation by P450s, then it is further bioactivated by NATs or SULTs to form *N*-acetoxy or *N*-sulfoxy esters, which lead to the formation of dG-C8-PhIP through the nitrenium intermediate. 5-Methylchrysene undergoes epoxidation (P450s 1A1 and 1B1) followed by epoxide hydroxylation (epoxide hydrolase) on the bay-region phenyl ring, to form the corresponding *trans*-1,2-dihydrodiol-5-methylchrysene. A subsequent round of monooxygenation leads to the formation of *anti*-1,2-dihydrodiol-3,4-epoxide-5-methylchrysene, which can form a DNA adduct at the *N*²-atom of dG (dG-*N*²-5-methylchrysene-diolepoxide). Two pathways are involved in the DNA adduct formation of the bioactivated tamoxifen. In the first pathway, oxidation of the allylic ethyl side chain results in the formation of α -hydroxytamoxifen. The subsequent esterification catalyzed by SULTs leads to the reactive carbenium intermediate and the dG-*N*²- α -hydroxytamoxifen adduct. The second pathway involves aryl-oxidation of one of the phenyl rings to yield 4-hydroxytamoxifen quinone methide, a reactive electrophile that can form the DNA adducts. Both pathways lead to (*Z*)- or (*E*)-dG-*N*²-4-hydroxytamoxifen.

Rodents are often employed as experimental laboratory animals to study metabolism of hazardous chemicals, to screen for DNA adduct formation, and elucidate mechanisms of carcinogenesis [5]. The metabolism of carcinogens and their biological effects in animal models can differ from humans because of species differences in catalytic activities of phase I and II enzymes involved in bioactivation or detoxification [10,16–18]. Thus, animal carcinogen bioassay data may not accurately gauge health risk of some chemicals in humans. However, DNA adducts of carcinogens, which are measures of the biologically effective dose, can serve as biomarkers for the extrapolation of genotoxicity data from animal studies for human risk assessment [19,20].

Epidemiological studies have reported that exposures to different chemicals in the diet and environment, or lifestyle factors, such as tobacco usage and alcohol consumption, are linked to the increased risk of developing certain types of cancers. As examples, polycyclic aromatic hydrocarbons (PAHs) in cigarette smoke are linked to lung cancer [21]; occupational exposures to aromatic amines are linked to bladder cancer [21,22]; usage of traditional Chinese herbal medicines containing AA-I are linked to upper urothelial cancer [23,24]; and consumption of aflatoxin B₁ (AFB₁) produced by fungi on agricultural crops, is a risk factor for liver cancer [25,26].

The identification and quantitation of DNA adducts is a first step in elucidating the potential role of a genotoxic chemical in the etiology of cancer [19,20]. The identification DNA adducts in human tissues are likely to represent a combination of recent and longer-term exposures to certain hazardous chemicals. The interpretation of negative findings, or the absence of DNA adducts, must be done with caution, since many adducts can undergo repair [27]. Ideally, the biomonitoring of DNA adducts should be conducted when the multistage process of tumorigenesis began, rather than many years later when the cancer is diagnosed. However, life-style factors such as tobacco smoking, diet, and environmental pollution often represent long-term exposures, and current adduct levels of carcinogens from these exposures are likely to correlate with adduct levels that existed during the time of tumor initiation and progression.

1.2. Methods to Measure DNA Adducts

The measurement of DNA adducts in humans is a challenging analytical task because the levels of DNA adducts generally occur at less than one adduct per 10⁷ nucleotides, and the amount of tissue available for measurement is limited. Even for blood, a readily accessible biofluid, the amount of DNA obtained is usually a few up to several tens of micrograms scale. Thus, highly sensitive and specific methods are required to measure DNA adducts in humans. During the past three decades, the major techniques employed to measure DNA adducts have been ³²P-postlabeling [28,29], antibody-based immunoassay/immunohistochemistry

(IHC) [30,31], gas chromatography-mass spectrometry (GC-MS) [32], and most recently, liquid chromatography-mass spectrometry (LC-MS) [33–37].

³²P-postlabeling is a highly sensitive method to detect DNA adducts. The DNA is enzymatically digested to 3'-phospho-2'-deoxyribonucleotides, and ³²P-orthophosphate from [γ -³²P] ATP is transferred to the 5'-OH position of the 2'-deoxyribonucleotide adduct, by polynucleotide kinase. The adducted 5'-³²P-labeled nucleotides are resolved by multi-dimensional thin-layer chromatography with polyethylenimine-modified cellulose plate, or by polyacrylamide electrophoresis, using autoradiography for detection, or by HPLC with radiometric detection [28,29,38,39]. The assay only requires 1–10 μ g of DNA, and the sensitivity for some adducts can reach a limit of detection as low as one adduct per 10¹⁰ nucleotides [29]. Studies in rodents and humans employing ³²P-postlabeling methods have shown that many genotoxic chemicals undergo metabolism and covalently adduct to DNA in many organs [29,40,41]. However, there are several limitations of the ³²P-postlabeling assay. The technique is labor intensive and its usage requires large amounts of hazardous phosphorous radioactivity. Moreover, the technique is not quantitative [42], and structural information about the identity of the adduct is uncertain, particularly in humans where many overlapping lesions are present [29,40]. Thus, epidemiology studies employing ³²P-postlabeling often provide equivocal data about chemical exposures linked to DNA adducts and cancer risk [43–46].

Immunodetection relies on the generation of monoclonal or polyclonal antibodies raised against modified-DNA adducts coupled to carrier proteins, or carcinogen-treated DNA, where usually very high levels of modification, about one modified base to 100 nucleotides, are required for successful generation of a titer [30,47]. The sensitivity of the method depends on the affinity of the antibody, but a detection limit of about one adduct per 10⁸ nucleotides for certain DNA adducts can be reached, when detected by fluorescence or chemiluminescence spectroscopy [48,49]. IHC detection of DNA adducts in tissue section-cuts mounted on slides is generally less sensitive than immunoassays performed on isolated DNA; however, IHC allows the visualization of the DNA adduct within specific cell types of a tissue, and is especially suitable for archived human formalin-fixed paraffin-embedded (FFPE) tissues (Section 3) [50]. Cross-reaction of the antibody with DNA adducts of similar structure or cellular components can occur [30,31], which raises concerns about the specificity of the methodology. Immunodetection methods have made significant contributions to the biomonitoring of DNA adducts; however, similarly to the ³²P-postlabeling method, immunodetection does not provide structural information to confirm adduct identity, and the method is semi-quantitative.

GC-MS with electron impact ionization, and more recently, negative ion chemical ionization has been employed to measure DNA adducts (primarily used for oxidized DNA bases) where adduct structures can be corroborated from the MS fragmentation spectra [32]. Often, the DNA is hydrolyzed with formic acid or by elevated temperature under neutral pH conditions. Most DNA adducts require chemical derivatization to increase the volatility required for GC analysis. The derivatization process can complicate the analysis and introduce artifact formation, particularly for oxidized DNA base measurements [51]. In contrast, the online coupling of capillary electrophoresis or LC to electrospray ionization (ESI) MS is a breakthrough technology that can measure many DNA adducts which would otherwise undergo thermal decomposition by GC-MS [52].

Currently, LC-ESI-multistage MS (MSⁿ) is the predominant platform for DNA adduct analyses [33,35,37,53]. The rapidly advancing technologies in LC-MS instrumentation have attained ultra-high sensitivity and selectivity, particularly with ion trap and high resolution accurate mass spectrometry (HRAMS). These platforms include the coupling of nano-flow chromatography and nanoESI source, and versatile and flexible scanning strategies. The detection of DNA adducts at levels as low as one per 10¹¹ nucleotides have been reported using a hybrid Orbitrap MS [54]. Both targeted and non-targeted MS scan approaches have been employed to identify many DNA chemical modifications [35–37,55–58].

The DNA is typically digested with a cocktail of nucleases prior to adduct measurements by LC-MS. The digestion products contain adducts formed at the DNA bases of the

2'-deoxyribonucleosides, or in rarer cases, adducts are formed at the phosphate backbones [59,60]. A common feature for many DNA adducts is their tendency to lose the deoxyribose moiety (dR, 116 or 116.0473 Da in HRAMS), when subjected to collision-induced dissociation (CID) [61]. The transition between the adduct precursors ($[M + H]^+$) and their aglycones after losing dR ($[M + H - 116]^+$) is commonly targeted to detect and quantify DNA adducts in MSⁿ. The constant neutral loss of molecules, such as dR from the 2'-deoxyribonucleosides, serves as the foundation of the "DNA adductomics" approach [37,55,56,62,63]. Figure 2 shows the fragmentation pathways of modified nucleosides, where the major ions are the chemically modified bases after neutral loss of dR, or in less frequent cases the bases are eliminated as the neutral fragment and the carcinogen moieties retain the charge. These types of MS transitions are usually monitored in the targeted and un-targeted approaches by LC-MS [58,63].

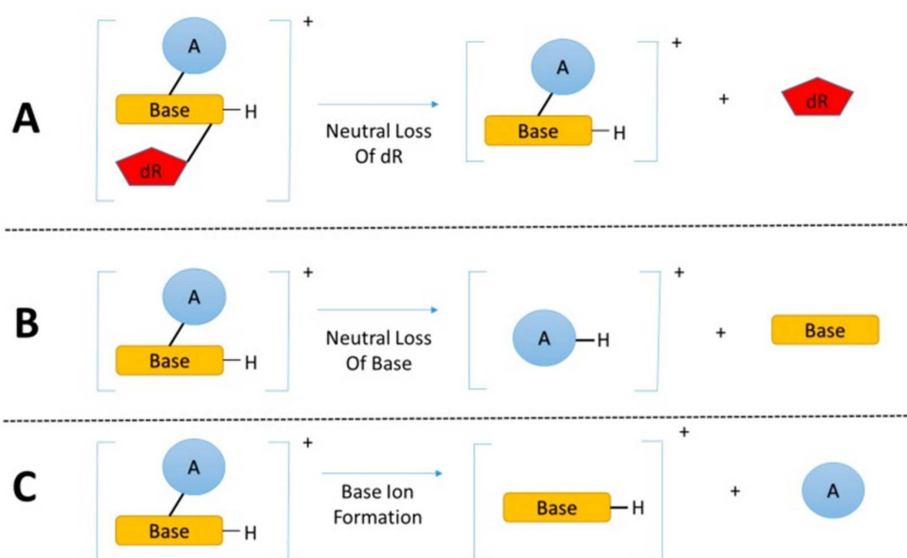


Figure 2. The fragmentation pathways of modified nucleosides analyzed by LC-MS. (A) The major fragmentation of the modified nucleosides is the neutral loss of deoxyribose. Other common fragmentations include (B) the neutral loss of base and (C) the neutral loss of the adduct with the formation of base ions [58].

2. Overview and the History of Formalin Fixation Process

While great strides have been made in the detection of DNA adducts in humans, fresh tissues obtained from biopsies or post-mortem are often not available. The paucity of fresh tissue specimens has hampered the advancement of DNA adduct biomonitoring in human studies. However, archived FFPE tissue specimens with clinical diagnosis of disease are a largely untapped biospecimen and often available for DNA adduct biomarker research.

Formalin, 10% neutral buffered formaldehyde solution, is the most commonly used fixative worldwide [64]. During the process of formalin fixation, formaldehyde undergoes multiple steps of reactions with cellular nucleophilic species to form molecular crosslinks [64,65]. Formaldehyde permeates through the tissue, and the nucleophilic moieties of amino acids and nucleobases attack the formaldehyde yielding unstable intermediates of methylol adducts and Schiff bases [65]. These intermediates are stabilized by forming methylene bridges with a second nucleophilic group, often on another molecule. The methylene bridges formed with DNA and protein are stable crosslinks at room temperature (Figure 3); however, the linkages are reversible by heat treatment and/or under alkaline pH [66,67]. The reversal rate of the crosslink increases exponentially as a function of temperature [66]. The efficacy of reversal of formaldehyde-mediated crosslinks is

the most critical feature that impacts the quantitative analysis of RNA, DNA, and protein biomarkers in FFPE tissues.

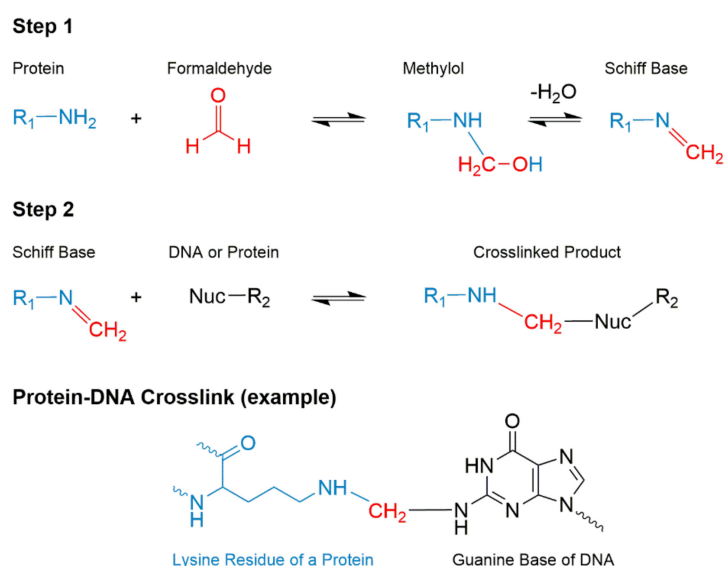


Figure 3. The reactions of formaldehyde mediated crosslinking of DNA and protein. Formaldehyde diffuses through tissue and reacts with a nucleophilic sites of protein and/or DNA base resulting in unstable intermediates of methylol and Schiff base. Then, a second nucleophile from inter- or intramolecular DNA or protein attacks the Schiff base resulting in a crosslinked complex. A specific example of a protein-DNA crosslink is shown. The atoms are color coded: cyan, protein; red, formaldehyde; and black, DNA. Reproduced with permission from [65]. Copyright ASBMB, 2015.

Technical Challenges and Breakthrough Technology in DNA Recovery from FFPE Tissues

FFPE tissues are now widely used in high throughput genomic [64,68–71], proteomics [72–74], and to a lesser extent, metabolomics studies [75,76]. The crucial step in these applications is the quantitative extraction of the molecules of interest. In genomic sequencing studies, the conventional method of DNA isolation from FFPE tissues has often employed elevated temperature (up to 100 °C) and alkaline pH (>9) to achieve a complete reversal of crosslinks. Many automated methods employed in cancer genomics still use elevated temperature to isolate DNA from FFPE tissues. The recovered DNA can serve as a template for PCR amplification. However, these harsh conditions can cause oxidation of nucleobases or depurination of chemically-modified nucleobases, and thus, are not compatible for quantitative measurements of DNA adducts. Moreover, even though formalin-fixation is the most common method of tissue preservation world-wide, the conditions of fixation can vary in different laboratories. A prolonged time of tissue preservation in formalin results in over-fixation of the tissue and leads to inefficient hydrolysis of crosslinks between DNA and protein. Therefore, the yield and quality of the recovered DNA is decreased [77–79]. Thus, the development of robust analytical methods to quantitatively recover DNA adducts from FFPE tissue has been a challenging endeavor.

3. Measurement of DNA Adducts in FFPE Tissues by IHC, ³²P-Postlabeling, and LC-MS

3.1. IHC Detection of DNA Adducts

FFPE specimens are often used for immunodetection of DNA adducts, most commonly by IHC methods [30,80]. In contrast to mass spectrometry-based methods, which break down the DNA to the mono 2'-deoxyribonucleoside or DNA base (*vide supra*), IHC methods employ intact DNA. The detection of DNA damage can be carried out on either fixed cells such as lymphocytes, exfoliated oral or bladder cells, or with FFPE tissue section-cuts. The cells or FFPE tissue section-cuts are mounted

on glass slides for IHC analysis. Procedures are often used to increase the accessibility of the antibody to the carcinogen DNA adduct to increase the sensitivity of the assay. These procedures can include treatment with proteases to remove histone and other proteins from the DNA, followed by treatment with RNase to eliminate potential cross-reactivity with RNA adducts. Mild acid or base treatment also may be performed to denature the DNA and further increase the accessibility of the antibody to the adduct. It is imperative that the adduct is stable to the denaturing treatment conditions for validation of the IHC technique. The two most commonly used detection systems for visualization of DNA adduct-antibody complexes are immunofluorescence or chromophores, where the secondary antibody is tagged with a chemically conjugated fluorophore, a peroxidase or alkaline phosphatase enzyme. [30,81].

Table 1 summarizes examples of IHC detection of DNA adducts in FFPE tissues. Santella's group detected and quantified DNA adducts of 4-aminobiphenyl (4-ABP), an aromatic amine and a human bladder carcinogen that is formed in tobacco smoke [21,22], and also occurs as a contaminant in some commercial hair dyes [82]. 4-ABP-adducted DNA was detected in uroepithelium of bladder cancer patients [83]. The level of the 4-ABP adduct was correlated with the smoking status and *p53* overexpression, a response to DNA damage. There was linear relationship between the relative degree of DNA adduct staining and the number of cigarettes smoked. The same group also detected DNA adducts of polycyclic aromatic hydrocarbons (PAHs) in archived breast tissues sections using polyclonal antiserum [84,85]. PAHs are incomplete combustion products of organic matter and found in cereal and grain products, some oils, and also found in charred meat and tobacco smoke [42]. PAHs have been linked to human cancers at multiple sites [21]. The most well studied PAH is benzo[*a*]pyrene (B[*a*]P), a human lung carcinogen found as an environmental pollutant, and it also occurs in tobacco smoke, and charred meat [42,86]. The Poirier laboratory developed an antibody raised against DNA modified with *7,8*-dihydroxy-*t*-9,10-oxy-7,8,9,10-tetrahydrobenzo[*a*]pyrene (BPDE) [87], which later was shown to cross-react with other structurally similar diol-epoxide-PAH-DNA adducts [88]. This PAH-DNA antiserum has been used to screen for DNA adducts in FFPE tissues from human esophagus [81,89], prostate [90], cervix [91], vulva [47], and placenta [80]. A significantly higher level of staining of presumed B[*a*]P adducts was found in benign breast disease in comparison to the cancerous tissues of patients, possibly due to cellular proliferation and dilution of the adduct in cancerous tissue [84,85]. Rundle et al. employed IHC to measure PAH-DNA adducts and examined the associations with alcohol consumption and the influence of GSTM1 genotype on DNA adduct formation in FFPE breast tissues [92]. Subjects harboring the GSTM1-null genotype, which lacks the expression of GSTM1, an enzyme that detoxicates PAH diol-epoxides [93], had increased levels of DNA adducts among current alcohol consumers, but not among nondrinkers. In contrast, in benign tissues from controls, no association was observed between genotype and adduct levels, regardless of drinking status. Poirier also analyzed tamoxifen-DNA adducts in rat hepatocytes by IHC [94]. A steady increase in adduct levels was observed with chronic exposure.

Shirai et al. developed polyclonal antibodies against DNA adducts of 3,2'-dimethyl-4-aminobiphenyl (DMAB), an aromatic amine that induces tumors at multiple sites in rodent models, and PhIP, a probable human carcinogen formed in cooked meat that induces tumors in colorectum and prostate of rodents [95–97]. Dose-related nuclear staining was observed in various acetone-fixed tissues of rodents 24 h after single exposure of DMAB or PhIP. Using the same polyclonal serum, putative DNA adducts of PhIP were detected, by IHC, at high frequency in mammary tissue of women with breast cancer [98] and in prostate tissue of men with prostate cancer [99]. However, these results are at odds with specific mass spectrometry-based methods, where PhIP DNA adducts were detected at considerably lower frequency and at much lower levels of DNA modification in both tissues [100,101]. The discrepancy between the estimates of the PhIP DNA adduct reported by MS and IHC methods suggest the possible cross-reactivity of the polyclonal antibodies with other DNA adducts of similar structure or endogenous cellular components. There is a need to cross-corroborate the identities and levels of DNA adducts measured by IHC and specific MS-based methods. Aoshiba

and coworkers raised antibodies against 8-hydroxy-2'-deoxyguanosine (8-OHdG), an oxidative DNA adduct, and 4-hydroxy-2-nonenal (4-HNE), a lipid peroxidation adduct, to evaluate the oxidative stress induced by cigarette smoke in paraffin-embedded pulmonary epithelial cells of mice [102]. There was a dramatic increase in the intensity of signals one hour post cigarette smoke exposure, compared to pre-exposure, which confirmed the causal role of cigarette smoking in oxidative damage to respiratory epithelium.

Table 1. Examples of DNA adducts detected in FFPE tissues.

| Detection Methods | DNA Adducts Detected | Tissues | LOD (Per 10 ⁸ Nucleotides) | References |
|------------------------------|---|--|---------------------------------------|------------|
| IHC | 4-ABP-DNA | Human bladder | NR ^a | [83] |
| | | Human breast | NR ^a | [84,85,92] |
| | | Human esophagus | NR ^a | [81,89] |
| | PAH-DNA | Human prostate | 8 | [90] |
| | | Human cervix | 20 | [91] |
| | | Human vulva | 8 | [47] |
| | | Human placenta | 20 | [80] |
| | DMAB-DNA | Rat multiple tissues | NR ^a | [96] |
| | PhIP-DNA | Human prostate tissue transplanted to mice | NR ^b | [96] |
| | | Rat multiple tissues | NR ^b | [97] |
| 8-OHdG | Mouse pulmonary epithelial cells | NR ^a | [102] | |
| Tamoxifen-DNA | Rat hepatocytes | 10 | [94] | |
| ³² P-postlabeling | B[a]P-DNA, 2-AAF-DNA | Rat multiple tissues | NR ^c | [103] |
| LC-MS ³ | dA-AL-I | Mouse liver and kidney, human kidney | 0.1 | [79,104] |
| | dG-C8-4-ABP/PhIP, dG-N ² -BPDE, O ⁶ -Me-dG and O ⁶ -POB-dG | Rodent multiple tissues | 0.2–0.5 | [105] |
| LC-HR-MS ² | dG-C8-PhIP | Human prostate | 0.13 | [101] |
| | dG-C8-4-ABP | Human bladder | 0.2 | [55] |

^a Adduct levels were reported as relative nuclear stain intensity; ^b Adduct levels were reported as a percentage of positive cells; ^c LOD was reported in the citation, which was one per 10¹⁰ nucleotides employing 10 µg DNA. NR: Not reported.

3.2. DNA Measurements in FFPE Tissues by ³²P-Postlabeling

There is only one report employing ³²P-postlabeling to detect DNA adducts in FFPE tissues [103]. In that study, rat tissues were fixed in formalin and embedded in paraffin after dosing with B[a]P or 2-acetylaminofluorene (2-AAF). DNA was extracted from fixed tissues using a modified phenol-chloroform method [106]. The levels of DNA adduct recovered from FFPE tissues were significantly lower than the levels obtained from fresh frozen tissues. The authors concluded that FFPE tissues could be used to screen for DNA adducts but that adduct levels may be underestimated particularly with prolonged time of fixation in formalin.

3.3. Measurement of DNA Adducts in FFPE Tissues of Rodents and Human by LC-MS

The physio-chemical data provided by MS for proof of DNA adduct structure combined with the robust quantitation and high sensitivity makes MS the technique of choice for DNA adduct biomarker measurements. The DNA adducts must be stable towards both the formalin fixation and DNA retrieval processes. Furthermore, the DNA must be fully digestible by nucleases to monodeoxyribonucleosides. Until recently, the recovery of high quality DNA completely devoid of formalin crosslinks was difficult to achieve under mild hydrolysis conditions. However, commercial kits from several vendors now employ mild retrieval conditions at neutral pH to reverse the crosslinks of FFPE DNA. The DNA recovered was shown to be successfully employed as templates for

amplification by PCR. We tested commercial kits from several vendors and found the FFPE miniprep kit from Zymo Research (Irvine, CA, USA), with some modifications in manufacturer's protocol, provided high quality DNA that was fully digestible by nucleases [79,101,105].

Our laboratory established a method to isolate DNA from FFPE liver and kidney tissues of C57BL/6J mice, using aristolochic acid I (AA-I) as the model carcinogen [79,104]. AA-I is an upper urinary tract human carcinogen found in Aristolochia plants, some of which have been used in traditional Chinese herbal medicines [79,104]. DNA was isolated from freshly frozen tissue by the phenol-chloroform method, and DNA from FFPE tissue was isolated with the FFPE miniprep kit (Zymo Research). AA-I DNA adducts were measured by ultra-performance liquid chromatography-electrospray ionization-ion trap-multistage MSⁿ scanning (UPLC-ESI-IT-MS³). Across all dosing levels, the amounts of AA-I DNA adduct in DNA from FFPE tissues were comparable to those of matching freshly frozen tissues (Figure 4) [104].

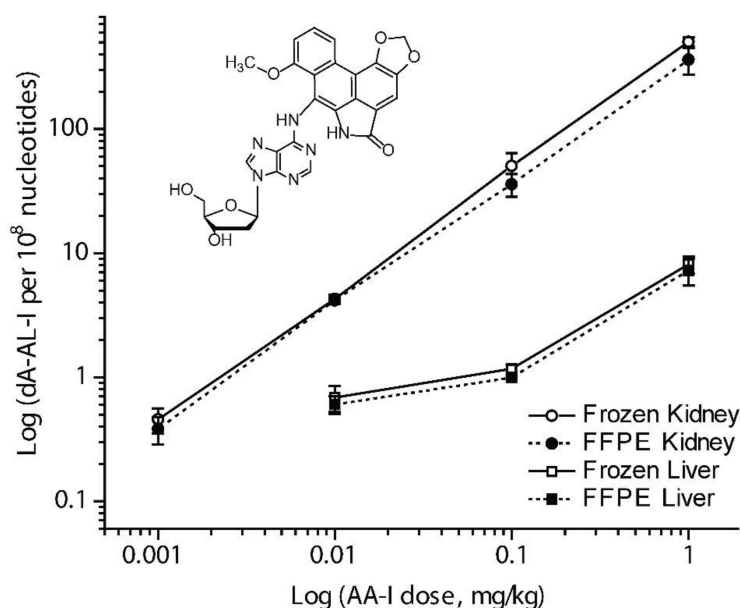


Figure 4. Mean level of dA-AL-I adducts present in mouse kidney and liver following treatment with AA-I (0.001–1 mg/kg body weight). Adduct levels measured in freshly frozen and FFPE mouse kidney (○ and ●) and liver (□ and ■) (mean adduct level, SD, $N = 4$ animals per dose, quadruplicate measurements per animal) were plotted as a function of dose. The overall mean difference in adduct levels between freshly frozen and FFPE kidney and liver tissues across all doses was $21 \pm 14\%$ (mean \pm SD). dA-AL-I adduct formation was below the limit of detection in liver of mice dosed with AA-I at 0.001 mg/kg body weight. Mean levels of dA-AL-I adducts were significantly statistically different between freshly frozen and FFPE kidney or liver at the following dose treatments of AA-I: kidney, 1 mg/kg, $p = 0.03$; liver, 0.1 mg/kg, $p = 0.01$; unpaired two-tailed t -test. Reproduced with permission from [104]. Copyright ACS, 2013.

Then, we examined the effect of duration of formalin fixation on the recovery of DNA and the level of DNA adducts in rodents treated with AA-I [79]. The yield of DNA retrieved from formalin-fixed tissues decreased as a function of fixation time, and only 30% of DNA was recovered from FFPE tissues after one week of fixation in formalin compared to the freshly frozen tissues. However, the DNA retrieved was completely digested by nucleases and the levels of AA-I DNA adduct were relatively constant between the freshly frozen tissues and FFPE tissues. DNA fragments of 184 and 327 bp extracted from FFPE tissues were readily amplified by PCR, and the quality of sequence data was comparable to that obtained from DNA obtained of fresh frozen tissues [79]. Our findings demonstrate that the DNA can be recovered from FFPE tissue to analyze DNA adducts of AA-I in FFPE tissue,

and adducts of AA-I or other carcinogens may be correlated with mutational signatures induced in tumor tissue.

Thereafter, we sought to determine if our method of DNA adduct retrieval from FFPE tissues could be employed to measure DNA adducts of other environmental and dietary genotoxicants. We examined DNA adducts of four important classes of environmental and dietary carcinogens: PAHs (B[a]P), aromatic amines (4-ABP), HAAs (PhIP), and *N*-nitroso compounds 4-(methylnitrosamino)-1-(3-pyridyl)-1-butanone (NNK), which is found in tobacco and a lung carcinogen [21,107]. The major DNA adducts of these carcinogens studied were: 10-(2'-deoxyguanosin-*N*²-yl)-7,8,9-trihydroxy-7,8,9,10-tetrahydrobenzo[*a*]pyrene (dG-*N*²-B[a]PPDE), *N*-(2'-deoxyguanosin-8-yl)-4-ABP (dG-C8-4-ABP), *N*-(2'-deoxyguanosin-8-yl)-PhIP (dG-C8-PhIP), O⁶-[4-oxo-4-(3-pyridyl)-butyl]-2'-deoxyguanosine (O⁶-POB-dG), O⁶-methyl-2'-deoxyguanosine (O⁶-methyl-dG) (Figure 5) [105]. All of these adducts and dA-AL-I were measured by UPLC-ESI-IT-MS³ with the stable isotope dilution method. The levels of DNA adducts in FFPE tissues of rodents preserved in formalin for 24 h were at levels comparable to those levels measured in freshly frozen tissues [105].

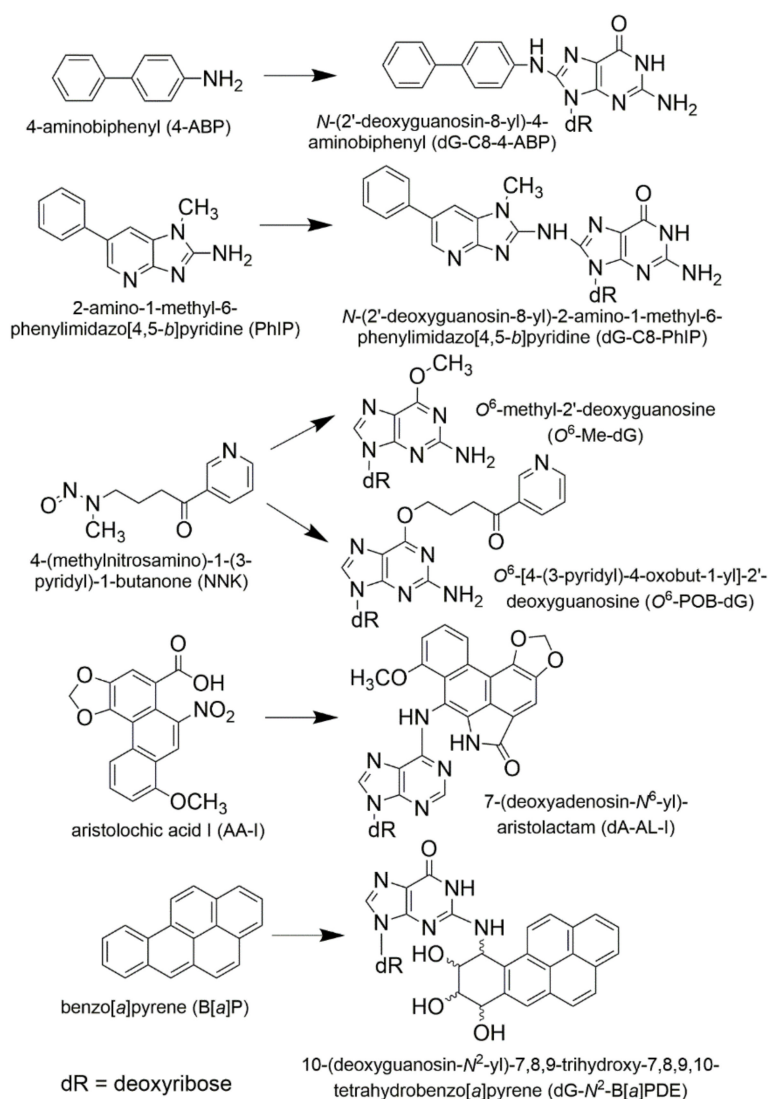


Figure 5. Structures, names, and abbreviations of carcinogens and their adducts used for quantitation of multiclass carcinogenic DNA adducts in freshly frozen and FFPE tissues of rodents. Reproduced with permission from [105]. Copyright ACS, 2016.

The recent improvements in sensitivity of mass spectrometry instrumentation has allowed us to use only 10 to 20 mg of tissue to screen for DNA adducts of environmental and dietary carcinogens in human biopsy samples [100,101,104]. We sought to determine if DNA extraction kits devoted to genomics, such as the FFPE miniprep kit from Zymo Research, could be employed to screen for DNA adducts in human FFPE biospecimens. We applied the method of DNA isolation to assay tissue section-cuts of human FFPE kidney specimens ($1.5 \text{ cm}^2 \times 10 \text{ }\mu\text{m}$) from the patients with upper urinary tract carcinoma, who were exposed to AA-I [79,104]. The levels of AA-I DNA adduct measured in FFPE tissues were comparable to those of matching frozen tissues (Figure 6). Some of these FFPE blocks had been stored at room temperature for four to nine years. This was the first report of quantitative measurement of a carcinogen DNA adduct in human FFPE tissue by mass spectrometry. We subsequently showed that DNA adducts of PhIP can be recovered in high yield from human FFPE prostate tissue blocks of prostate cancer patients stored at room temperature for at least 6 months (Figure 7) [101,108]. These findings show that FFPE tissues can be used to retrospectively screen for multiple classes of carcinogen DNA adducts.

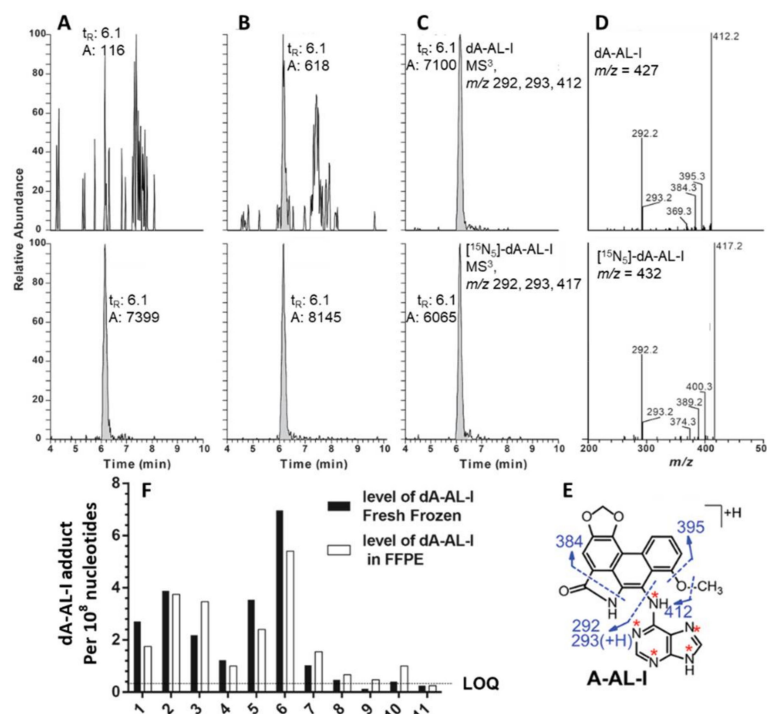


Figure 6. Extracted ion chromatograms of dA-AL-I from human kidney cortex of patients with upper urothelial cancer from Taiwan at levels (A) below the LOQ, and positive samples at (B) 0.4 adducts, and (C) 5.9 adducts per 10^8 bases. The product ion spectra of dA-AL-I obtained from panel C is depicted in (D) along with the internal standard $[^{15}\text{N}_5]$ -dA-AL-I (E, ^{15}N labels of the internal standard of dA-AL-I are depicted with asterisks). Insert (F) dA-AL-I adduct levels in matching fresh frozen and FFPE kidney samples, containing both renal cortex and medulla, obtained from 11 individuals residing in endemic regions of Croatia and Serbia who underwent nephroureterectomy for upper urothelial cancer. Reproduced with permission from [104]. Copyright ACS, 2013.

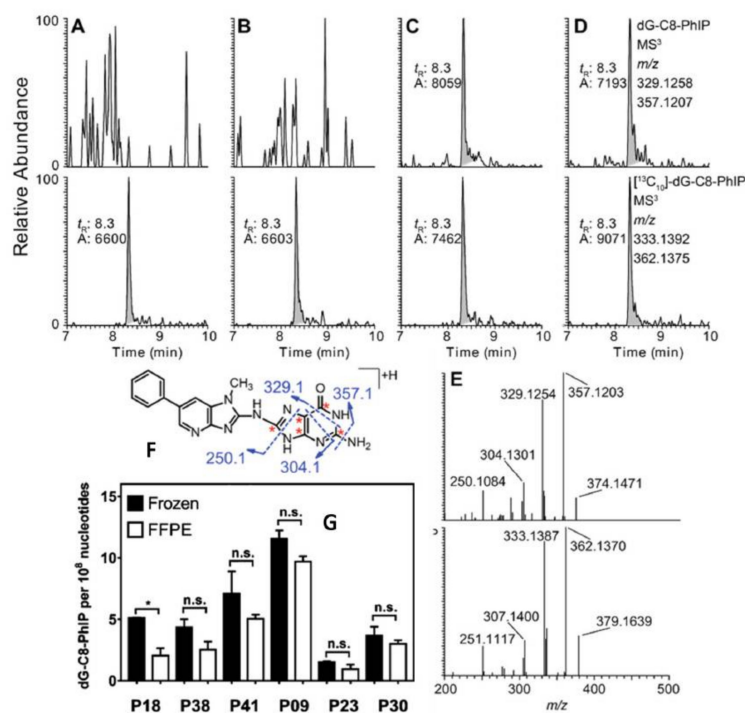


Figure 7. Extracted ion chromatograms of dG-C8-PhIP and ¹³C-labeled dG-C8-PhIP of DNA from fresh frozen and FFPE human prostate tissues at the MS³ scan stage. (A) Fresh frozen prostate and (B) paired FFPE block of a patient who was negative for dG-C8-PhIP; (C) fresh frozen prostate and (D) paired FFPE block of a patient who was positive dG-C8-PhIP at MS³ scan stage. The structure and proposed fragmentation mechanism of aglycone of dG-C8-PhIP are depicted fresh frozen prostate and (D) paired FFPE block of a patient who was positive for dG-C8-PhIP. (E) The product ion spectra at MS³ of unlabeled and ¹³C-labeled dG-C8-PhIP are shown. (F) Levels of dG-C8-PhIP in paired fresh frozen prostate and FFPE blocks of six patients are shown in (G). The levels of adducts are reported as adducts per 10⁸ nucleotides. * $p < 0.05$; n.s., statistically not significant. Reproduced with permission from [108]. Copyright ACS, 2017.

3.4. Rapid Throughput Method of DNA Extraction from FFPE Tissue

The method of DNA isolation from FFPE tissues employing the FFPE miniprep kit (Zymo Research) is robust; however, it is a manual and labor-intensive technique and cannot readily process the large number of samples required for epidemiological studies. We developed a rapid throughput method of DNA isolation from FFPE tissue employing a semi-automated commercial DNA isolation system, Promega Maxwell[®] 16 MDx system, which is used for genomic research [108]. The system employs silica-magnetic beads technology for DNA isolation and can process 32 samples per hour compared to 4–6 samples per hour by the manual method. The DNA recovered from FFPE tissues using the Promega Maxwell[®] 16 MDx is fully digestible by nucleases [108]. The levels of dA-AL-I, dG-C8-4-ABP, and dG-C8-PhIP recovered from DNA of FFPE tissues extracted by rapid throughput method are comparable to those levels measured from DNA isolated by phenol-chloroform in matching frozen tissues, and in DNA of FFPE tissues isolated by the commercial manual Zymo kit [108]. With this advancement in DNA isolation technology, we believe that archived FFPE tissues can be used to screen for DNA adducts in large population studies. A scheme and the time of duration of the procedure to isolate DNA from FFPE section cuts or whole tissues, and ensuing chemical analysis by mass spectrometry, are depicted in Figure 8. The recovery of DNA from FFPE tissues and DNA digestion steps require overnight incubation with enzymes to achieve optimal digestion efficiency. The targeted and simultaneous quantification of a selected number of DNA adducts, by UPLC-ESI-IT-MS³, can be achieved in a 10 to 15 min run time.

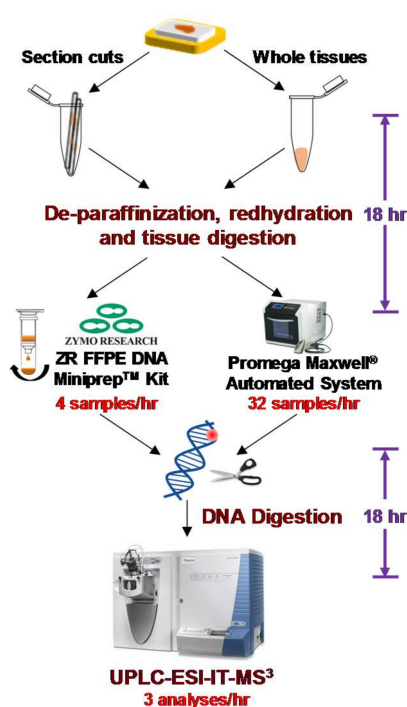


Figure 8. Scheme of FFPE tissue processing for DNA adduct measurements. DNA is extracted from section cuts or excised whole tissues by the FFPE Miniprep kit (Zymo Research) or Promega Maxwell® automated system. After nuclease digestion, the DNA adducts are measured by UPLC-ESI-IT-MS³. The estimated times of the different processes are reported.

3.5. Future Applications of DNA Adduct Measurements in Human Tissues

Although this review has focused on DNA adducts of environmental and dietary carcinogens, the measurements of DNA adducts of chemotherapeutic agents, such as platinum drugs and nitrogen mustards used to treat cancer, also can be measured in fresh frozen and FFPE tissues by mass spectrometry. Drugs that modify the structure of DNA and target cancer cells by interfering with DNA synthesis and cell replication often remain first line of medications used in cancer treatment. Thus, the efficacy of many anticancer drugs is thought to be linked to the levels of specific DNA adducts formed during drug treatment, and the quantitative measurements of the DNA adducts may be used as predictive markers in precision medicine to identify individuals who are most likely to benefit from treatment from those patients who may be less responsive to the therapy [109]. The assessment of DNA adducts of chemotherapeutic drugs and their cellular biological responses has been mostly performed in surrogate specimens, such as white blood cells or in vitro using cell lines rather than in the target cells or tumors, because of the invasiveness of biopsy sampling [109]. However, the exquisite sensitivity of current mass spectrometry instrumentation can allow for measurements that characterize the relationships between level of anticancer drug DNA adducts and pharmacodynamic response in patients using only 10 mg of tissue. As the sensitivity of MS instrumentation continues to improve, the amount of tissue specimen required for analysis will be further reduced, and the application of DNA adduct monitoring of chemotherapeutic drugs in clinical settings can be achieved.

The screening of DNA from FFPE tissues shows great promise to measure DNA adducts of multiple classes of carcinogens and anticancer drugs [37,55,105,109]. While most analyses have focused on one to several adducts, different types of MS scanning approaches are being developed to simultaneous scan for multiple types of DNA adducts in the field of DNA adductomics [63]. Triple quadrupole, quadrupole time-of-flight, ion trap or Orbitrap mass spectrometry instrumentation are being employed in DNA adductomics [55,58,62,63,110]. Our laboratory is developing unbiased non-targeted ion trap and Orbitrap scanning methods to screen for an array of DNA adducts in the

human genome in a single assay [55,58]. Some of these adducts are expected to contribute to the tumor mutation burden [111].

A critical need is the development of accompanying informatic tools for data analysis and statistical tools to screen for covalent DNA damage. These scanning technologies and accompanying data analysis tools will provide a wealth of information about the exogenous and endogenous chemicals that damage the genome and may contribute to cancer risk. The implementation of FFPE tissues in DNA adduct biomarker discovery can provide the clues about the origin of human cancers for which an environmental exposure is suspected.

Author Contributions: All authors critically reviewed the literature and contributed to drafting the manuscript.

Acknowledgments: The work cited in this review conducted by the Turesky laboratory has been supported by Grants R01ES019564 and R21ES014438 from the National Institute of Environmental Health Sciences, R01CA122320, R01CA220367, and R33CA186795, and the National Center for Advancing Translational Sciences award number UL1TR000114 from the National Cancer Institute of the National Institutes of Health. Mass spectrometry was carried out in Analytical Biochemistry Shared Resources of the Masonic Cancer Center, University of Minnesota, funded in part by Cancer Center Support Grant CA-077598.

Conflicts of Interest: The authors declare no conflict of interest.

References

1. Stanley, L.A. Drug Metabolism. In *Pharmacognosy: Fundamentals, Applications and Strategies*; Badal, S., Delgado, R., Eds.; Elsevier: London, UK, 2017; pp. 527–545.
2. Guengerich, F.P. Cytochrome p450 and chemical toxicology. *Chem. Res. Toxicol.* **2008**, *21*, 70–83. [[CrossRef](#)] [[PubMed](#)]
3. Grillo, M.P. Bioactivation by Phase-II-Enzyme-Catalyzed Conjugation of Xenobiotics. In *Encyclopedia of Drug Metabolism and Interactions*; Lyubimov, A.V., Ed.; Wiley: Hoboken, NJ, USA, 2012; Volume 4.
4. Dekant, W. The role of biotransformation and bioactivation in toxicity. In *Molecular, Clinical and Environmental Toxicology*; Luch, A., Ed.; Birkhäuser: Basel, Switzerland, 2009; Volume 1, pp. 57–86.
5. Miller, E.C. Some current perspectives on chemical carcinogenesis in humans and experimental animals: Presidential address. *Cancer Res.* **1978**, *38*, 1479–1496. [[PubMed](#)]
6. Minchin, R.F.; Reeves, P.T.; Teitel, C.H.; McManus, M.E.; Mojarrabi, B.; Ilett, K.F.; Kadlubar, F.F. N- and O-acetylation of aromatic and heterocyclic amine carcinogens by human monomorphic and polymorphic acetyltransferases expressed in COS-1 cells. *Biochem. Biophys. Res. Commun.* **1992**, *185*, 839–844. [[CrossRef](#)]
7. Thier, R.; Pemble, S.E.; Kramer, H.; Taylor, J.B.; Guengerich, F.P.; Ketterer, B. Human glutathione S-transferase T1-1 enhances mutagenicity of 1,2-dibromoethane, dibromomethane and 1,2,3,4-diepoxybutane in Salmonella typhimurium. *Carcinogenesis* **1996**, *17*, 163–166. [[CrossRef](#)] [[PubMed](#)]
8. Fu, P.P.; Miller, D.W.; Von Tungeln, L.S.; Bryant, M.S.; Lay, J.O., Jr.; Huang, K.; Jones, L.; Evans, F.E. Formation of C8-modified deoxyguanosine and C8-modified deoxyadenosine as major DNA adducts from 2-nitropyrene metabolism mediated by rat and mouse liver microsomes and cytosols. *Carcinogenesis* **1991**, *12*, 609–616. [[CrossRef](#)] [[PubMed](#)]
9. Regan, S.L.; Maggs, J.L.; Hammond, T.G.; Lambert, C.; Williams, D.P.; Park, B.K. Acyl glucuronides: The good, the bad and the ugly. *Biopharm. Drug Dispos.* **2010**, *31*, 367–395. [[CrossRef](#)] [[PubMed](#)]
10. Nauwelaers, G.; Bessette, E.E.; Gu, D.; Tang, Y.; Rageul, J.; Fessard, V.; Yuan, J.M.; Yu, M.C.; Langouet, S.; Turesky, R.J. DNA adduct formation of 4-aminobiphenyl and heterocyclic aromatic amines in human hepatocytes. *Chem. Res. Toxicol.* **2011**, *24*, 913–925. [[CrossRef](#)] [[PubMed](#)]
11. Sidorenko, V.S.; Attaluri, S.; Zaitseva, I.; Iden, C.R.; Dickman, K.G.; Johnson, F.; Grollman, A.P. Bioactivation of the human carcinogen aristolochic acid. *Carcinogenesis* **2014**, *35*, 1814–1822. [[CrossRef](#)] [[PubMed](#)]
12. Reardon, D.B.; Prakash, A.S.; Hilton, B.D.; Roman, J.M.; Pataki, J.; Harvey, R.G.; Dipple, A. Characterization of 5-methylchrysene-1,2-dihydrodiol-3,4-epoxide-DNA adducts. *Carcinogenesis* **1987**, *8*, 1317–1322. [[CrossRef](#)] [[PubMed](#)]
13. Penning, T.M. The aldo-keto reductases (AKRs): Overview. *Chem. Biol. Interact.* **2015**, *234*, 236–246. [[CrossRef](#)] [[PubMed](#)]

14. Marques, M.M.; Beland, F.A. Identification of tamoxifen-DNA adducts formed by 4-hydroxytamoxifen quinone methide. *Carcinogenesis* **1997**, *18*, 1949–1954. [[CrossRef](#)] [[PubMed](#)]
15. Osborne, M.R.; Hewer, A.; Hardcastle, I.R.; Carmichael, P.L.; Phillips, D.H. Identification of the major tamoxifen-deoxyguanosine adduct formed in the liver DNA of rats treated with tamoxifen. *Cancer Res.* **1996**, *56*, 66–71. [[PubMed](#)]
16. Guengerich, F.P. Comparisons of catalytic selectivity of cytochrome P450 subfamily enzymes from different species. *Chem. Biol. Interact.* **1997**, *106*, 161–182. [[CrossRef](#)]
17. Turesky, R.J.; Constable, A.; Fay, L.B.; Guengerich, F.P. Interspecies differences in metabolism of heterocyclic aromatic amines by rat and human P450 1A2. *Cancer Lett.* **1999**, *143*, 109–112. [[CrossRef](#)]
18. Edwards, R.J.; Murray, B.P.; Murray, S.; Schulz, T.; Neubert, D.; Gant, T.W.; Thorgeirsson, S.S.; Boobis, A.R.; Davies, D.S. Contribution of CYP1A1 and CYP1A2 to the activation of heterocyclic amines in monkeys and humans. *Carcinogenesis* **1994**, *15*, 829–836. [[CrossRef](#)] [[PubMed](#)]
19. Himmelstein, M.W.; Boogaard, P.J.; Cadet, J.; Farmer, P.B.; Kim, J.H.; Martin, E.A.; Persaud, R.; Shuker, D.E. Creating context for the use of DNA adduct data in cancer risk assessment: II. Overview of methods of identification and quantitation of DNA damage. *Crit. Rev. Toxicol.* **2009**, *39*, 679–694. [[CrossRef](#)] [[PubMed](#)]
20. Jarabek, A.M.; Pottenger, L.H.; Andrews, L.S.; Casciano, D.; Embry, M.R.; Kim, J.H.; Preston, R.J.; Reddy, M.V.; Schoeny, R.; Shuker, D.; et al. Creating context for the use of DNA adduct data in cancer risk assessment: I. Data organization. *Crit. Rev. Toxicol.* **2009**, *39*, 659–678. [[CrossRef](#)] [[PubMed](#)]
21. IARC. Tobacco smoke and involuntary smoking. *IARC Monogr. Eval. Carcinog. Risks Hum.* **2004**, *83*, 1–1438.
22. IARC. Tobacco smoking. *IARC Monogr. Eval. Carcinog. Risks Hum.* **1986**, *38*, 35–394.
23. Stiborova, M.; Arlt, V.M.; Schmeiser, H.H. DNA Adducts Formed by Aristolochic Acid Are Unique Biomarkers of Exposure and Explain the Initiation Phase of Upper Urothelial Cancer. *Int. J. Mol. Sci.* **2017**, *18*, 2144. [[CrossRef](#)] [[PubMed](#)]
24. Rosenquist, T.A.; Grollman, A.P. Mutational signature of aristolochic acid: Clue to the recognition of a global disease. *DNA Repair* **2016**, *44*, 205–211. [[CrossRef](#)] [[PubMed](#)]
25. Wogan, G.N.; Kensler, T.W.; Groopman, J.D. Present and future directions of translational research on aflatoxin and hepatocellular carcinoma. A review. *Food Addit. Contam. Part A Chem. Anal. Control Expo. Risk Assess.* **2012**, *29*, 249–257. [[CrossRef](#)] [[PubMed](#)]
26. Kensler, T.W.; Roebuck, B.D.; Wogan, G.N.; Groopman, J.D. Aflatoxin: A 50-year odyssey of mechanistic and translational toxicology. *Toxicol. Sci.* **2011**, *120* (Suppl. 1), S28–S48. [[CrossRef](#)] [[PubMed](#)]
27. Sancar, A.; Lindsey-Boltz, L.A.; Unsal-Kacmaz, K.; Linn, S. Molecular mechanisms of mammalian DNA repair and the DNA damage checkpoints. *Annu. Rev. Biochem.* **2004**, *73*, 39–85. [[CrossRef](#)] [[PubMed](#)]
28. Randerath, K.; Reddy, M.V.; Gupta, R.C. ³²P-labeling test for DNA damage. *Proc. Natl. Acad. Sci. USA* **1981**, *78*, 6126–6129. [[CrossRef](#)] [[PubMed](#)]
29. Phillips, D.H. On the origins and development of the (32)P-postlabelling assay for carcinogen-DNA adducts. *Cancer Lett.* **2013**, *334*, 5–9. [[CrossRef](#)] [[PubMed](#)]
30. Santella, R.M. Immunological methods for detection of carcinogen-DNA damage in humans. *Cancer Epidemiol. Biomark. Prev.* **1999**, *8*, 733–739.
31. Poirier, M.C.; Santella, R.M.; Weston, A. Carcinogen macromolecular adducts and their measurement. *Carcinogenesis* **2000**, *21*, 353–359. [[CrossRef](#)] [[PubMed](#)]
32. Dizdaroglu, M.; Coskun, E.; Jaruga, P. Measurement of oxidatively induced DNA damage and its repair, by mass spectrometric techniques. *Free Radic. Res.* **2015**, *49*, 525–548. [[CrossRef](#)] [[PubMed](#)]
33. Singh, R.; Farmer, P.B. Liquid chromatography-electrospray ionization-mass spectrometry: The future of DNA adduct detection. *Carcinogenesis* **2006**, *27*, 178–196. [[CrossRef](#)] [[PubMed](#)]
34. Klaene, J.J.; Sharma, V.K.; Glick, J.; Vouros, P. The analysis of DNA adducts: The transition from (32)P-postlabeling to mass spectrometry. *Cancer Lett.* **2013**, *334*, 10–19. [[CrossRef](#)] [[PubMed](#)]
35. Liu, S.; Wang, Y. Mass spectrometry for the assessment of the occurrence and biological consequences of DNA adducts. *Chem. Soc. Rev.* **2015**, *44*, 7829–7854. [[CrossRef](#)] [[PubMed](#)]
36. Tretyakova, N.; Goggin, M.; Sangaraju, D.; Janis, G. Quantitation of DNA adducts by stable isotope dilution mass spectrometry. *Chem. Res. Toxicol.* **2012**, *25*, 2007–2035. [[CrossRef](#)] [[PubMed](#)]
37. Guo, J.; Turesky, R.J. Human Biomonitoring of DNA Adducts by Ion Trap Multistage Mass Spectrometry. *Curr. Protoc. Nucleic Acid Chem.* **2016**, *66*, 7.24.21–7.24.25. [[PubMed](#)]

38. Shibutani, S.; Kim, S.Y.; Suzuki, N. ³²P-Postlabeling DNA damage assays: PAGE, TLC, and HPLC. *Methods Mol. Biol.* **2006**, *314*, 307–321. [[PubMed](#)]
39. Pfau, W.; Lecoq, S.; Hughes, N.C.; Seidel, A.; Platt, K.L.; Grover, P.L.; Phillips, D.H. Separation of ³²P-labelled nucleoside 3',5'-bisphosphate adducts by HPLC. *IARC Sci. Publ.* **1993**, 233–242.
40. Phillips, D.H. DNA adducts as markers of exposure and risk. *Mutat. Res.* **2005**, *577*, 284–292. [[CrossRef](#)] [[PubMed](#)]
41. Phillips, D.H. Smoking-related DNA and protein adducts in human tissues. *Carcinogenesis* **2002**, *23*, 1979–2004. [[CrossRef](#)] [[PubMed](#)]
42. Phillips, D.H. Polycyclic aromatic hydrocarbons in the diet. *Mutat. Res.* **1999**, *443*, 139–147. [[CrossRef](#)]
43. Agudo, A.; Peluso, M.; Munnia, A.; Lujan-Barroso, L.; Sanchez, M.J.; Molina-Montes, E.; Sanchez-Cantalejo, E.; Navarro, C.; Tormo, M.J.; Chirlaque, M.D.; et al. Aromatic DNA adducts and risk of gastrointestinal cancers: A case-cohort study within the EPIC-Spain. *Cancer Epidemiol. Biomark. Prev.* **2012**, *21*, 685–692. [[CrossRef](#)] [[PubMed](#)]
44. Gilbertson, T.; Peluso, M.E.; Munia, A.; Lujan-Barroso, L.; Sanchez, M.J.; Navarro, C.; Amiano, P.; Barricarte, A.; Quiros, J.R.; Molina-Montes, E.; et al. Aromatic adducts and lung cancer risk in the European Prospective Investigation into Cancer and Nutrition (EPIC) Spanish cohort. *Carcinogenesis* **2014**, *35*, 2047–2054. [[CrossRef](#)] [[PubMed](#)]
45. Ricceri, F.; Godschalk, R.W.; Peluso, M.; Phillips, D.H.; Agudo, A.; Georgiadis, P.; Loft, S.; Tjonneland, A.; Raaschou-Nielsen, O.; Palli, D.; et al. Bulky DNA adducts in white blood cells: A pooled analysis of 3600 subjects. *Cancer Epidemiol. Biomark. Prev.* **2010**, *19*, 3174–3181. [[CrossRef](#)] [[PubMed](#)]
46. Ho, V.; Peacock, S.; Massey, T.E.; Godschalk, R.W.; van Schooten, F.J.; Chen, J.; King, W.D. Gene-diet interactions in exposure to heterocyclic aromatic amines and bulky DNA adduct levels in blood leukocytes. *Environ. Mol. Mutagen.* **2015**, *56*, 609–620. [[CrossRef](#)] [[PubMed](#)]
47. Pratt, M.M.; John, K.; MacLean, A.B.; Afework, S.; Phillips, D.H.; Poirier, M.C. Polycyclic aromatic hydrocarbon (PAH) exposure and DNA adduct semi-quantitation in archived human tissues. *Int. J. Environ. Res. Public Health* **2011**, *8*, 2675–2691. [[CrossRef](#)] [[PubMed](#)]
48. Mumford, J.L.; Williams, K.; Wilcosky, T.C.; Everson, R.B.; Young, T.L.; Santella, R.M. A sensitive color ELISA for detecting polycyclic aromatic hydrocarbon-DNA adducts in human tissues. *Mutat. Res.* **1996**, *359*, 171–177. [[CrossRef](#)]
49. Divi, R.L.; Beland, F.A.; Fu, P.P.; Von Tungeln, L.S.; Schoket, B.; Camara, J.E.; Ghei, M.; Rothman, N.; Sinha, R.; Poirier, M.C. Highly sensitive chemiluminescence immunoassay for benzo[a]pyrene-DNA adducts: Validation by comparison with other methods, and use in human biomonitoring. *Carcinogenesis* **2002**, *23*, 2043–2049. [[CrossRef](#)] [[PubMed](#)]
50. Poirier, M.C. Chemical-induced DNA damage and human cancer risk. *Nat. Rev. Cancer* **2004**, *4*, 630–637. [[CrossRef](#)] [[PubMed](#)]
51. Ravanat, J.L.; Turesky, R.J.; Gremaud, E.; Trudel, L.J.; Stadler, R.H. Determination of 8-oxoguanine in DNA by gas chromatography-mass spectrometry and HPLC-electrochemical detection: Overestimation of the background level of the oxidized base by the gas chromatography-mass spectrometry assay. *Chem. Res. Toxicol.* **1995**, *8*, 1039–1045. [[CrossRef](#)] [[PubMed](#)]
52. Turesky, R.J.; Vouros, P. Formation and analysis of heterocyclic aromatic amine-DNA adducts in vitro and in vivo. *J. Chromatogr. B Anal. Technol. Biomed. Life Sci.* **2004**, *802*, 155–166. [[CrossRef](#)] [[PubMed](#)]
53. Tretyakova, N.; Villalta, P.W.; Kotapati, S. Mass spectrometry of structurally modified DNA. *Chem. Rev.* **2013**, *113*, 2395–2436. [[CrossRef](#)] [[PubMed](#)]
54. Villalta, P.W.; Hochalter, J.B.; Hecht, S.S. Ultrasensitive High-Resolution Mass Spectrometric Analysis of a DNA Adduct of the Carcinogen Benzo[a]pyrene in Human Lung. *Anal. Chem.* **2017**, *89*, 12735–12742. [[CrossRef](#)] [[PubMed](#)]
55. Guo, J.; Villalta, P.W.; Turesky, R.J. Data-Independent Mass Spectrometry Approach for Screening and Identification of DNA Adducts. *Anal. Chem.* **2017**, *89*, 11728–11736. [[CrossRef](#)] [[PubMed](#)]
56. Bessette, E.E.; Goodenough, A.K.; Langouet, S.; Yasa, I.; Kozekov, I.D.; Spivack, S.D.; Turesky, R.J. Screening for DNA adducts by data-dependent constant neutral loss-triple stage mass spectrometry with a linear quadrupole ion trap mass spectrometer. *Anal. Chem.* **2009**, *81*, 809–819. [[CrossRef](#)] [[PubMed](#)]

57. Balbo, S.; Hecht, S.S.; Upadhyaya, P.; Villalta, P.W. Application of a high-resolution mass-spectrometry-based DNA adductomics approach for identification of DNA adducts in complex mixtures. *Anal. Chem.* **2014**, *86*, 1744–1752. [[CrossRef](#)] [[PubMed](#)]
58. Villalta, P.W.; Balbo, S. The Future of DNA Adductomic Analysis. *Int. J. Mol. Sci.* **2017**, *18*, 1870. [[CrossRef](#)]
59. Ma, B.; Zarth, A.T.; Carlson, E.S.; Villalta, P.W.; Upadhyaya, P.; Stepanov, I.; Hecht, S.S. Methyl DNA Phosphate Adduct Formation in Rats Treated Chronically with 4-(Methylnitrosamino)-1-(3-pyridyl)-1-butanone and Enantiomers of Its Metabolite 4-(Methylnitrosamino)-1-(3-pyridyl)-1-butanol. *Chem. Res. Toxicol.* **2018**, *31*, 48–57. [[CrossRef](#)] [[PubMed](#)]
60. Ma, B.; Zarth, A.T.; Carlson, E.S.; Villalta, P.W.; Stepanov, I.; Hecht, S.S. Pyridylhydroxybutyl and pyridyloxobutyl DNA phosphate adduct formation in rats treated chronically with enantiomers of the tobacco-specific nitrosamine metabolite 4-(methylnitrosamino)-1-(3-pyridyl)-1-butanol. *Mutagenesis* **2017**, *32*, 561–570. [[CrossRef](#)] [[PubMed](#)]
61. Wolf, S.M.; Vouros, P. Application of capillary liquid chromatography coupled with tandem mass spectrometric methods to the rapid screening of adducts formed by the reaction of *N*-acetoxy-*N*-acetyl-2-aminofluorene with calf thymus DNA. *Chem. Res. Toxicol.* **1994**, *7*, 82–88. [[CrossRef](#)] [[PubMed](#)]
62. Kanaly, R.A.; Matsui, S.; Hanaoka, T.; Matsuda, T. Application of the adductome approach to assess intertissue DNA damage variations in human lung and esophagus. *Mutat. Res.* **2007**, *625*, 83–93. [[CrossRef](#)] [[PubMed](#)]
63. Balbo, S.; Turesky, R.J.; Villalta, P.W. DNA adductomics. *Chem. Res. Toxicol.* **2014**, *27*, 356–366. [[CrossRef](#)] [[PubMed](#)]
64. Fox, C.H.; Johnson, F.B.; Whiting, J.; Roller, P.P. Formaldehyde fixation. *J. Histochem. Cytochem.* **1985**, *33*, 845–853. [[CrossRef](#)] [[PubMed](#)]
65. Hoffman, E.A.; Frey, B.L.; Smith, L.M.; Auble, D.T. Formaldehyde crosslinking: A tool for the study of chromatin complexes. *J. Biol. Chem.* **2015**, *290*, 26404–26411. [[CrossRef](#)] [[PubMed](#)]
66. Kennedy-Darling, J.; Smith, L.M. Measuring the formaldehyde Protein-DNA cross-link reversal rate. *Anal. Chem.* **2014**, *86*, 5678–5681. [[CrossRef](#)] [[PubMed](#)]
67. Boenisch, T. Effect of heat-induced antigen retrieval following inconsistent formalin fixation. *Appl. Immunohistochem. Mol. Morphol.* **2005**, *13*, 283–286. [[CrossRef](#)] [[PubMed](#)]
68. Graw, S.; Meier, R.; Minn, K.; Bloomer, C.; Godwin, A.K.; Fridley, B.; Vlad, A.; Beyerlein, P.; Chien, J. Robust gene expression and mutation analyses of RNA-sequencing of formalin-fixed diagnostic tumor samples. *Sci. Rep.* **2015**, *5*, 12335. [[CrossRef](#)] [[PubMed](#)]
69. Ludgate, J.L.; Wright, J.; Stockwell, P.A.; Morison, I.M.; Eccles, M.R.; Chatterjee, A. A streamlined method for analysing genome-wide DNA methylation patterns from low amounts of FFPE DNA. *BMC Med. Genom.* **2017**, *10*, 54. [[CrossRef](#)] [[PubMed](#)]
70. Robbe, P.; Popitsch, N.; Knight, S.J.L.; Antoniou, P.; Becq, J.; He, M.; Kanapin, A.; Samsonova, A.; Vavoulis, D.V.; Ross, M.T.; et al. Clinical whole-genome sequencing from routine formalin-fixed, paraffin-embedded specimens: Pilot study for the 100,000 Genomes Project. *Genet. Med.* **2018**. [[CrossRef](#)] [[PubMed](#)]
71. Moran, S.; Vizoso, M.; Martinez-Cardus, A.; Gomez, A.; Matias-Guiu, X.; Chiavenna, S.M.; Fernandez, A.G.; Esteller, M. Validation of DNA methylation profiling in formalin-fixed paraffin-embedded samples using the Infinium HumanMethylation450 Microarray. *Epigenetics* **2014**, *9*, 829–833. [[CrossRef](#)] [[PubMed](#)]
72. Jiang, X.; Jiang, X.; Feng, S.; Tian, R.; Ye, M.; Zou, H. Development of efficient protein extraction methods for shotgun proteome analysis of formalin-fixed tissues. *J. Proteome Res.* **2007**, *6*, 1038–1047. [[CrossRef](#)] [[PubMed](#)]
73. Sprung, R.W.; Brock, J.W.C.; Tanksley, J.P.; Li, M.; Washington, M.K.; Slebos, R.J.C.; Liebler, D.C. Equivalence of Protein Inventories Obtained from Formalin-fixed Paraffin-embedded and Frozen Tissue in Multidimensional Liquid Chromatography-Tandem Mass Spectrometry Shotgun Proteomic Analysis. *Mol. Cell. Proteom.* **2009**, *8*, 1988–1998. [[CrossRef](#)] [[PubMed](#)]
74. Giusti, L.; Lucacchini, A. Proteomic studies of formalin-fixed paraffin-embedded tissues. *Expert Rev. Proteom.* **2013**, *10*, 165–177. [[CrossRef](#)] [[PubMed](#)]

75. Kelly, A.D.; Breitkopf, S.B.; Yuan, M.; Goldsmith, J.; Spentzos, D.; Asara, J.M. Metabolomic profiling from formalin-fixed, paraffin-embedded tumor tissue using targeted LC/MS/MS: Application in sarcoma. *PLoS ONE* **2011**, *6*, e25357. [[CrossRef](#)] [[PubMed](#)]
76. Wojakowska, A.; Chekan, M.; Marczak, L.; Polanski, K.; Lange, D.; Pietrowska, M.; Widlak, P. Detection of metabolites discriminating subtypes of thyroid cancer: Molecular profiling of FFPE samples using the GC/MS approach. *Mol. Cell. Endocrinol.* **2015**, *417*, 149–157. [[CrossRef](#)] [[PubMed](#)]
77. Mortensen, E.; Brown, J. Effects of Fixation on Tissues. In *Prostate Cancer Methods and Protocols*; Russell, P., Jackson, P., Kingsley, E., Eds.; Springer: New York, NY, USA, 2003; Volume 81, pp. 163–179.
78. Xie, R.; Chung, J.Y.; Ylaya, K.; Williams, R.L.; Guerrero, N.; Nakatsuka, N.; Badie, C.; Hewitt, S.M. Factors influencing the degradation of archival formalin-fixed paraffin-embedded tissue sections. *J. Histochem. Cytochem.* **2011**, *59*, 356–365. [[CrossRef](#)] [[PubMed](#)]
79. Yun, B.H.; Yao, L.; Jelakovic, B.; Nikolic, J.; Dickman, K.G.; Grollman, A.P.; Rosenquist, T.A.; Turesky, R.J. Formalin-fixed paraffin-embedded tissue as a source for quantitation of carcinogen DNA adducts: Aristolochic acid as a prototype carcinogen. *Carcinogenesis* **2014**, *35*, 2055–2061. [[CrossRef](#)] [[PubMed](#)]
80. Pratt, M.M.; King, L.C.; Adams, L.D.; John, K.; Sirajuddin, P.; Olivero, O.A.; Manchester, D.K.; Sram, R.J.; DeMarini, D.M.; Poirier, M.C. Assessment of multiple types of DNA damage in human placentas from smoking and nonsmoking women in the Czech Republic. *Environ. Mol. Mutagen.* **2011**, *52*, 58–68. [[CrossRef](#)] [[PubMed](#)]
81. Van Gijssel, H.E.; Divi, R.L.; Olivero, O.A.; Roth, M.J.; Wang, G.Q.; Dawsey, S.M.; Albert, P.S.; Qiao, Y.L.; Taylor, P.R.; Dong, Z.W.; et al. Semiquantitation of polycyclic aromatic hydrocarbon-DNA adducts in human esophagus by immunohistochemistry and the automated cellular imaging system. *Cancer Epidemiol. Biomark. Prev.* **2002**, *11*, 1622–1629.
82. Turesky, R.J.; Freeman, J.P.; Holland, R.D.; Nestorick, D.M.; Miller, D.W.; Ratnasinghe, D.L.; Kadlubar, F.F. Identification of aminobiphenyl derivatives in commercial hair dyes. *Chem. Res. Toxicol.* **2003**, *16*, 1162–1173. [[CrossRef](#)] [[PubMed](#)]
83. Curigliano, G.; Zhang, Y.J.; Wang, L.Y.; Flamini, G.; Alcini, A.; Ratto, C.; Giustacchini, M.; Alcini, E.; Cittadini, A.; Santella, R.M. Immunohistochemical quantitation of 4-aminobiphenyl-DNA adducts and p53 nuclear overexpression in T1 bladder cancer of smokers and nonsmokers. *Carcinogenesis* **1996**, *17*, 911–916. [[CrossRef](#)] [[PubMed](#)]
84. Santella, R.M.; Gammon, M.D.; Zhang, Y.J.; Motykiewicz, G.; Young, T.L.; Hayes, S.C.; Terry, M.B.; Schoenberg, J.B.; Brinton, L.A.; Bose, S.; et al. Immunohistochemical analysis of polycyclic aromatic hydrocarbon-DNA adducts in breast tumor tissue. *Cancer Lett.* **2000**, *154*, 143–149. [[CrossRef](#)]
85. Motykiewicz, G.; Malusecka, E.; Michalska, J.; Kalinowska, E.; Wloch, J.; Butkiewicz, D.; Mazurek, A.; Lange, D.; Perera, F.P.; Santella, R.M. Immunoperoxidase detection of polycyclic aromatic hydrocarbon-DNA adducts in breast tissue sections. *Cancer Detect. Prev.* **2001**, *25*, 328–335. [[PubMed](#)]
86. Hecht, S.S. Progress and challenges in selected areas of tobacco carcinogenesis. *Chem. Res. Toxicol.* **2008**, *21*, 160–171. [[CrossRef](#)] [[PubMed](#)]
87. Poirier, M.C.; Santella, R.; Weinstein, I.B.; Grunberger, D.; Yuspa, S.H. Quantitation of benzo(a)pyrene-deoxyguanosine adducts by radioimmunoassay. *Cancer Res.* **1980**, *40*, 412–416. [[PubMed](#)]
88. Weston, A.; Manchester, D.K.; Poirier, M.C.; Choi, J.S.; Trivers, G.E.; Mann, D.L.; Harris, C.C. Derivative fluorescence spectral analysis of polycyclic aromatic hydrocarbon-DNA adducts in human placenta. *Chem. Res. Toxicol.* **1989**, *2*, 104–108. [[CrossRef](#)] [[PubMed](#)]
89. Van Gijssel, H.E.; Schild, L.J.; Watt, D.L.; Roth, M.J.; Wang, G.Q.; Dawsey, S.M.; Albert, P.S.; Qiao, Y.L.; Taylor, P.R.; Dong, Z.W.; et al. Polycyclic aromatic hydrocarbon-DNA adducts determined by semiquantitative immunohistochemistry in human esophageal biopsies taken in 1985. *Mutat. Res.* **2004**, *547*, 55–62. [[CrossRef](#)] [[PubMed](#)]
90. John, K.; Ragavan, N.; Pratt, M.M.; Singh, P.B.; Al-Buheissi, S.; Matanhelia, S.S.; Phillips, D.H.; Poirier, M.C.; Martin, F.L. Quantification of phase I/II metabolizing enzyme gene expression and polycyclic aromatic hydrocarbon-DNA adduct levels in human prostate. *Prostate* **2009**, *69*, 505–519. [[CrossRef](#)] [[PubMed](#)]

91. Pratt, M.M.; Sirajuddin, P.; Poirier, M.C.; Schiffman, M.; Glass, A.G.; Scott, D.R.; Rush, B.B.; Olivero, O.A.; Castle, P.E. Polycyclic aromatic hydrocarbon-DNA adducts in cervix of women infected with carcinogenic human papillomavirus types: An immunohistochemistry study. *Mutat. Res.* **2007**, *624*, 114–123. [[CrossRef](#)] [[PubMed](#)]
92. Rundle, A.; Tang, D.L.; Mooney, L.; Grumet, S.; Perera, F. The interaction between alcohol consumption and GSTM1 genotype on polycyclic aromatic hydrocarbon-DNA adduct levels in breast tissue. *Cancer Epidemiol. Biomark. Prev.* **2003**, *12*, 911–914.
93. Bartsch, H.; Hietanen, E. The role of individual susceptibility in cancer burden related to environmental exposure. *Environ. Health Perspect.* **1996**, *104* (Suppl. 3), 569–577. [[CrossRef](#)] [[PubMed](#)]
94. Divi, R.L.; Dragan, Y.P.; Pitot, H.C.; Poirier, M.C. Immunohistochemical localization and semi-quantitation of hepatic tamoxifen-DNA adducts in rats exposed orally to tamoxifen. *Carcinogenesis* **2001**, *22*, 1693–1699. [[CrossRef](#)] [[PubMed](#)]
95. Felton, J.S.; Jagerstad, I.M.; Knize, M.G.; Skog, K.; Wakabayashi, K. Contents in Foods, Beverages and Tobacco. In *Food Borne Carcinogens: Heterocyclic Amines*; Nagao, M., Sugimura, T., Eds.; John Wiley & Sons Ltd.: Chichester, UK, 2000; pp. 31–71.
96. Shirai, T.; Takahashi, S.; Cui, L.; Yamada, Y.; Tada, M.; Kadlubar, F.F.; Ito, N. Use of polyclonal antibodies against carcinogen-DNA adducts in analysis of carcinogenesis. *Toxicol. Lett.* **1998**, *102–103*, 441–446. [[CrossRef](#)]
97. Takahashi, S.; Tamano, S.; Hirose, M.; Kimoto, N.; Ikeda, Y.; Sakakibara, M.; Tada, M.; Kadlubar, F.F.; Ito, N.; Shirai, T. Immunohistochemical demonstration of carcinogen-DNA adducts in tissues of rats given 2-amino-1-methyl-6-phenylimidazo[4,5-*b*]pyridine (PhIP): Detection in paraffin-embedded sections and tissue distribution. *Cancer Res.* **1998**, *58*, 4307–4313. [[PubMed](#)]
98. Zhu, J.; Chang, P.; Bondy, M.L.; Sahin, A.A.; Singletary, S.E.; Takahashi, S.; Shirai, T.; Li, D. Detection of 2-amino-1-methyl-6-phenylimidazo[4,5-*b*]pyridine-DNA adducts in normal breast tissues and risk of breast cancer. *Cancer Epidemiol. Biomark. Prev.* **2003**, *12*, 830–837.
99. Tang, D.; Liu, J.J.; Rundle, A.; Neslund-Dudas, C.; Saveria, A.T.; Bock, C.H.; Nock, N.L.; Yang, J.J.; Rybicki, B.A. Grilled meat consumption and PhIP-DNA adducts in prostate carcinogenesis. *Cancer Epidemiol. Biomarkers Prev.* **2007**, *16*, 803–808. [[CrossRef](#)] [[PubMed](#)]
100. Gu, D.; Turesky, R.J.; Tao, Y.; Langouet, S.A.; Nauwelaers, G.C.; Yuan, J.M.; Yee, D.; Yu, M.C. DNA adducts of 2-amino-1-methyl-6-phenylimidazo[4,5-*b*]pyridine and 4-aminobiphenyl are infrequently detected in human mammary tissue by liquid chromatography/tandem mass spectrometry. *Carcinogenesis* **2012**, *33*, 124–130. [[CrossRef](#)] [[PubMed](#)]
101. Xiao, S.; Guo, J.; Yun, B.H.; Villalta, P.W.; Krishna, S.; Tejpaul, R.; Murugan, P.; Weight, C.J.; Turesky, R.J. Biomonitoring DNA Adducts of Cooked Meat Carcinogens in Human Prostate by Nano Liquid Chromatography-High Resolution Tandem Mass Spectrometry: Identification of 2-Amino-1-methyl-6-phenylimidazo[4,5-*b*]pyridine DNA Adduct. *Anal. Chem.* **2016**, *88*, 12508–12515. [[CrossRef](#)] [[PubMed](#)]
102. Aoshiba, K.; Koinuma, M.; Yokohori, N.; Nagai, A. Immunohistochemical evaluation of oxidative stress in murine lungs after cigarette smoke exposure. *Inhal. Toxicol.* **2003**, *15*, 1029–1038. [[CrossRef](#)] [[PubMed](#)]
103. Hewer, A.; Phillips, D.H. Effect of tissue fixation on recovery of DNA adducts in the ³²P-postlabelling assay. *IARC Sci. Publ.* **1993**, 211–214.
104. Yun, B.H.; Rosenquist, T.A.; Nikolic, J.; Dragicevic, D.; Tomic, K.; Jelakovic, B.; Dickman, K.G.; Grollman, A.P.; Turesky, R.J. Human Formalin-Fixed Paraffin-Embedded Tissues: an untapped specimen for biomonitoring of carcinogen DNA adducts by mass spectrometry. *Anal. Chem.* **2013**, *85*, 4251–4258. [[CrossRef](#)] [[PubMed](#)]
105. Guo, J.; Yun, B.H.; Upadhyaya, P.; Yao, L.; Krishnamachari, S.; Rosenquist, T.A.; Grollman, A.P.; Turesky, R.J. Multiclass carcinogenic DNA adduct quantification in formalin-fixed paraffin-embedded tissues by ultraperformance liquid chromatography-tandem mass spectrometry. *Anal. Chem.* **2016**, *88*, 4780–4787. [[CrossRef](#)] [[PubMed](#)]
106. Goelz, S.E.; Hamilton, S.R.; Vogelstein, B. Purification of DNA from formaldehyde fixed and paraffin embedded human tissue. *Biochem. Biophys. Res. Commun.* **1985**, *130*, 118–126. [[CrossRef](#)]
107. IARC. Smokeless Tobacco and Some Tobacco-Specific N-Nitrosamines. *IARC Monogr. Eval. Carcinog. Risks Hum.* **2007**, *89*, 1–152.

108. Yun, B.H.; Xiao, S.; Yao, L.; Krishnamachari, S.; Rosenquist, T.A.; Dickman, K.G.; Grollman, A.P.; Murugan, P.; Weight, C.J.; Turesky, R.J. A rapid throughput method to extract DNA from formalin-fixed paraffin-embedded tissues for biomonitoring carcinogenic DNA adducts. *Chem. Res. Toxicol.* **2017**, *30*, 2130–2139. [[CrossRef](#)] [[PubMed](#)]
109. Stornetta, A.; Zimmermann, M.; Cimino, G.D.; Henderson, P.T.; Sturla, S.J. DNA adducts from anticancer drugs as candidate predictive markers for precision medicine. *Chem. Res. Toxicol.* **2017**, *30*, 388–409. [[CrossRef](#)] [[PubMed](#)]
110. Yao, C.; Feng, Y.L. A nontargeted screening method for covalent DNA adducts and DNA modification selectivity using liquid chromatography-tandem mass spectrometry. *Talanta* **2016**, *159*, 93–102. [[CrossRef](#)] [[PubMed](#)]
111. Stratton, M.R.; Campbell, P.J.; Futreal, P.A. The cancer genome. *Nature* **2009**, *458*, 719–724. [[CrossRef](#)] [[PubMed](#)]



© 2018 by the authors. Licensee MDPI, Basel, Switzerland. This article is an open access article distributed under the terms and conditions of the Creative Commons Attribution (CC BY) license (<http://creativecommons.org/licenses/by/4.0/>).